Center for Turbulence Research
Proceedings of the Summer Program 1988

Sensitivity of mixing layers to three-dimensional forcing

By J. J. Riley[1], P. D. Mourad[1], R. D. Moser[2] AND M. M. Rogers[2]

1. Introduction

It is well-known that turbulent mixing layers are dominated by large-scale, fairly coherent structures, and that these structures are related to the stability characteristics of the flow (see, for example, Ho & Huerre 1984, for an excellent review of this subject). These facts have led researchers to attempt controlling such flows by selectively forcing certain unstable modes, which can in addition have the effect of suppressing other modes. For example Oster & Wygnanski (1982) and Ho & Huang (1982) found that, by subjecting the mixing layer to oscillatory disturbances upstream of the splitter plate at frequencies related to unstable modes, the growth of the layer could be significantly inhibited. Similarly it has been found (Husain & Hussain 1986) that forcing at certain frequencies and their subharmonics can enhance the growth of the mixing layer.

Much of the work on controlling the mixing layer has relied on forcing two-dimensional instabilities. In this study we address the results of forcing three-dimensional instabilities. The objectives of our work are twofold: (1) to understand how a mixing layer responds to three-dimensional perturbations, and (2) to test the validity of an amplitude expansion in predicting the mixing layer development. The amplitude expansion could be very useful in understanding and predicting the three-dimensional response of the flow to a variety of initial conditions.

The mixing layer is sensitive to several aspects of the imposed perturbations, including their wavelength or frequency (see, *e.g.*, Michalke, 1964), the relative phases of the disturbances if more than one are used (*e.g.*, Patnaik, Sherman & Corcos 1976), the relative amplitudes of the disturbances (Metcalfe *et al.* 1987), and their shape (*e.g.*, eigenfunctions of the Orr-Sommerfeld equation, etc.). The approach we would like to take is to systematically explore the sensitivity of the mixing layer to various types of three-dimensional perturbations, using both direct numerical simulations and amplitude expansions. However, the potential parameter space to explore is very large. In this preliminary study we begin by selecting several different conditions for simulation and examining the behavior of the computed flow fields. In order to test the amplitude expansion technique, we compare previous simulation results with predictions from the theory for cases where the simulations and theory treat similar initial conditions. In this preliminary study, we limit the application of the expansion technique to two-dimensional mixing layers.

1 University of Washington
2 NASA Ames Research Center

C-2

2. Mathematical description

Consider a temporally evolving mixing layer with a Cartesian coordinate system oriented with x in the mean flow direction, y in the direction of the variation of the mean velocity, and z in the transverse direction.

It is both convenient and natural to consider initial perturbations of the form

$$u_i(x,y,z) = \tilde{u}_i(\alpha,y,\gamma)e^{i(\alpha x+\gamma z)}$$

since this is the form of the stability eigenfunctions. The simulations and analysis were performed using initial conditions consisting of the sum of a few perturbations of this form. Consider first the two-dimensional modes, where $\gamma = 0$. If the simulations were initialized at a very low level with broad-banded noise, then the first significant disturbance would appear at approximately $(\alpha_F, 0)$, where α_F is the wave number of the most unstable mode based upon linear stability theory ($\alpha_F \approx 0.8892\delta$, where δ is the initial vorticity thickness, Michalke, 1964). Initialization of this mode causes roll up to occur (Patnaik, Sherman & Corcos 1976; Riley & Metcalfe, 1980), and the development of higher harmonics (*e.g.*, $(2\alpha_F, 0)$). If the initial field is broad-banded, then the subharmonic $(1/2\,\alpha_F, 0)$ will also show significant growth, both due to its own inherent instability and also to nonlinear interaction with the fundamental. Vortex pairing will eventually occur. The behavior of these two-dimensional disturbances is well-documented by laboratory experiments, numerical simulations, and theory.

Next consider three-dimensional disturbances ($\gamma \neq 0$). In laboratory experiments used to study the mixing layer downstream of a splitter plate, it is observed that the initial primary three-dimensional disturbance consists of streamwise vortices of a particular wavelength (approximately $\gamma_F = 1.5\alpha_F$) that appear locked in phase (Bernal, 1981; Ho & Huang, 1982). In the current nomenclature, these modes are the points $(0, \gamma_F)$ in the (α, γ) plane. Initial disturbances of this type were considered by Pierrehumbert & Widnall (1982), and their growth termed translative instability. It was found that, based upon linear stability theory, these translative modes are weakly algebraically unstable. However, in the presence of a finite amplitude, two-dimensional disturbance, the translative modes become highly unstable.

Another mode that has received some previous attention is the oblique mode at (α_F, γ_F), which was addressed theoretically by Pierrehumbert & Widnall (1982) and Corcos & Lin (1984), and numerically by Metcalfe *et al.* (1987). The latter work showed that initializing these modes along with the fundamental results in streamwise disturbances very similar to those observed in the laboratory. This mode is unstable according to linear stability theory, but the quoted previous work shows that it is much more unstable in the presence of finite amplitude, two-dimensional disturbances.

At this point it is important to mention certain differences between the spatially-evolving and temporally-evolving mixing layers. The former is what is usually studied in laboratory experiments, and is a more realistic approximation to many flows encountered in technology, *e.g.*, in mixing regions in reaction chambers. The

temporally-evolving mixing layer is probably a better model for geophysical situations, *e.g.*, mixing layers in the atmosphere or oceans. It has been studied more often numerically because of the significant numerical advantages in avoiding inflow/outflow boundary conditions. Some laboratory experiments have been conducted for the temporally-evolving case (see, *e.g.*, Thorpe, 1985) using salt-stratified water in a tilting tank.

The temporal mixing layer studied in the tilting tank experiments shows little evidence of the strong streamwise vortices which are commonly observed in spatially-evolving mixing layers (Thorpe 1985). This is perhaps due to the fact that the $(0, \gamma_F)$ mode would not be preferentially excited in these experiments. In spatially-evolving mixing layer experiments, streamwise vortices are often present at the edge of the splitter plate, and are probably related to features of the particular experimental facility (Ho, 1988). Although the temporally-evolving flow exhibits the same qualitative two-dimensional features as the spatially-evolving mixing layer, *e.g.*, rollup and pairing, it appears that the development of the three-dimensional disturbances may be significantly different, due to differences in the nature of the disturbances. In the numerical simulations presented in §4, initial disturbances which would produce streamwise vortices similar to those observed in *spatially* developing mixing layers were selected.

To address the problem of the sensitivity of the mixing layer to three-dimensional disturbances, we consider the constant density Navier-Stokes equations:

$$\frac{\partial \mathbf{u}}{\partial t} + \mathbf{u} \cdot \nabla \mathbf{u} = -\nabla p + R^{-1} \nabla^2 \mathbf{u} \tag{2.1}$$

$$\nabla \cdot \mathbf{u} = 0 \tag{2.2}$$

Here $\mathbf{u} = (u, v, w)$ is the velocity vector and p is the pressure. The equations have been nondimensionalized using the velocity scale $\Delta U/2$, half the mean velocity difference across the layer; the length scale $\delta = \Delta U / U_y(y = 0)$ (initial vorticity thickness) and the time scale $2\delta/\Delta U$. The Reynolds number R is defined $R = \Delta U \delta / 2\nu$.

The initial velocity field consists of an initial mean velocity U plus an initial perturbation $\mathbf{u}'$. U is taken to be an error function, $(U(y) = \mathrm{erf}(\sqrt{\pi} y))$ For boundary conditions we assume periodicity in the x and z directions, and assume that all perturbations decay as $|y| \to \infty$.

3 Amplitude expansion technique

We have extended a procedure for theoretical analysis of two-dimensional wave-wave interactions in unstable shear flows (Mourad, 1987; Mourad & Brown, 1988) to the case of two- and three-dimensional waves, here applied to the temporal mixing layer. The details of this derivation and results are in the Appendix. As a first application to the mixing layer, we will consider the classic problem of the interaction of a two-dimensional wave with its two-dimensional subharmonic, to determine if we can reproduce the phase-dependency of their evolution, as described in Patnaik, Sherman & Corcos (1976), Riley & Metcalfe (1980) and Ho and Huerre (1984); see also Mansour *et al.* in this volume.

3.1 Two-dimensional amplitude expansions

We begin by listing the equations governing the temporal evolution for the stream function of the two dimensional fundamental, with amplitude and phase $A(t)$ and $\theta_A(t)$, respectively, and of the subharmonic, with amplitude and phase $B(t)$ and $\theta_B(t)$, respectively.

$$\frac{1}{A}\frac{dA}{dt} - i\frac{d}{dt}\theta_A = a_0 + a_1\frac{B^2}{A}e^{-i(2\theta_B-\theta_A)} + a_3A^2 + a_4B^2 \tag{2.3}$$

$$\begin{aligned}\frac{1}{B}\frac{dB}{dt} - i\frac{d}{dt}\theta_B = {} & b_0 + b_1Ae^{-i(\theta_A-2\theta_B)} + b_3A^2 + b_4B_2 \\ & + b_7A^2e^{-2i(\theta_A-2\theta_B)} + b_8A^2e^{-i(\theta_A-2\theta_B)}\cos(\theta_A - 2\theta_B) \\ & + b_9A^2e^{-i(\theta_A-2\theta_B)}\sin(\theta_A - 2\theta_B)\end{aligned} \tag{2.4}$$

As discussed in detail in the Appendix, the rational for these equations is similar to that of Lorenz, or of Stuart's energy method (Ho & Huerre, 1984). Like them, we derive Equations (2.3) and (2.4) without benefit of asymptotic analysis, which would ordinarily allow for an ordering of the weights of the various physical processes in the mixing layer. We forgo asymptotics, because a reasonable small parameter is not available for our use in supercritical mixing layers. Instead, the expansions are truncated based on the physical processes we wish to include or remove from the model. Finally, like Lorenz and Stuart, we hope that the results lend at least qualitative insight into the true physical processes. We do, however, include more detail in the expansions than these other theories.

In 2.3 and 2.4, a_0 and b_0 govern the linear growth of their respective disturbances. They are complex constants of the form $\sigma_p - \omega_p i$, where σ_p is the growth rate and ω_p is the linear frequency of each of the waves.

The terms beginning with a_1 and b_1 represent the effects of the changes induced by each wave on the other. This direct interaction was the focus of the asymptotic study of Monkewitz (1988), who used an expansion near the critical Reynolds number (≈ 0) to define a small parameter. However, for supercritical flows, other nonlinear effects are also important (see Ho & Huerre 1984). Only a_1 and b_1 terms are included by Monkewitz and others, because they show that when the flow is near critical the return-feedback effects discussed below occur on a much longer time scale than the initial interaction.

Next, the term with coefficient a_3 represents the affects on the fundamental wave of the modified mean flow and the first harmonic $(2\alpha_F, 0)$. Both the modified mean and the first harmonic are forced by the fundamental. This term generally acts to check the unbridled growth of the wave in a supercritical flow.

The term with a_4 represents a variety of physical effects. These include the effect on the fundamental of (1) the modification to the mean flow induced by the subharmonic wave; (2) the distortion of the subharmonic induced by the fundamental (as represented by the b_1 term). The energy methods would have a term like a_4 in their evolution equations which would not include the second contribution.

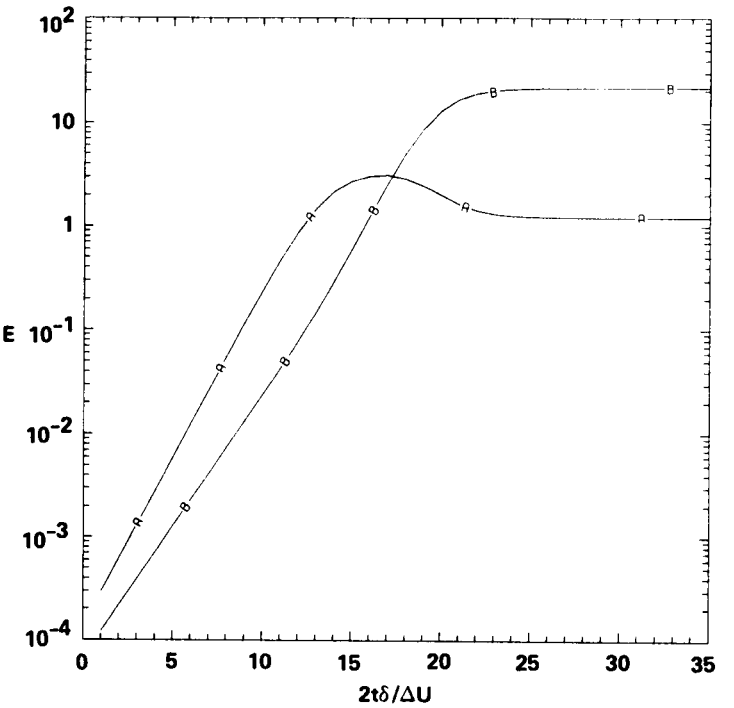

FIGURE 1. Evolution of the energy in the (A) fundamental ($E_{(\alpha_F,0)}$) and (B) subharmonic as predicted by equations (2.3) and (2.4).

The term beginning with b_3 represents the effects on the subharmonic of the changes in the mean flow induced by the fundamental, and the b_4 term is analogous to the a_3 term. In addition, b_4 includes additional effects due to the direct interaction of the fundamental and subharmonic, as in the a_4 term.

The more exotic looking terms with b_7, b_8 and b_9 are all due to the impact of the direct interaction of $(\alpha_F, 0)$ and $(\alpha_F/2, 0)$ on the subharmonic.

3.2 Two-dimensional amplitude expansion results

For this report, we will not consider a detailed discussion of the roles played by the various terms in the calculations; though this is of great interest, it is left for future work. Here we will verify the effect on the interactions of changing the initial phase difference between the fundamental and subharmonic. The importance of the relative phase is well documented (Husain & Hussain 1986, Patnaik, Sherman & Corcos 1976, and Riley & Metcalfe 1980). Following the definitions used in the numerical simulations, the fundamental and subharmonic are *in-phase* if alternate cores of the fundamental modes are aligned with the cores of the subharmonic modes. They are *out-of-phase* if the cores of the subharmonic are between the cores of the fundamental. (This is apparently opposite to the definition used in the review article of Ho & Huerre, 1984.) An operational definition like that above is important, since the linear stability eigenfunctions have an arbitrary phase.

Figure 1 shows a typical result of integrating the evolution equations (2.3 and

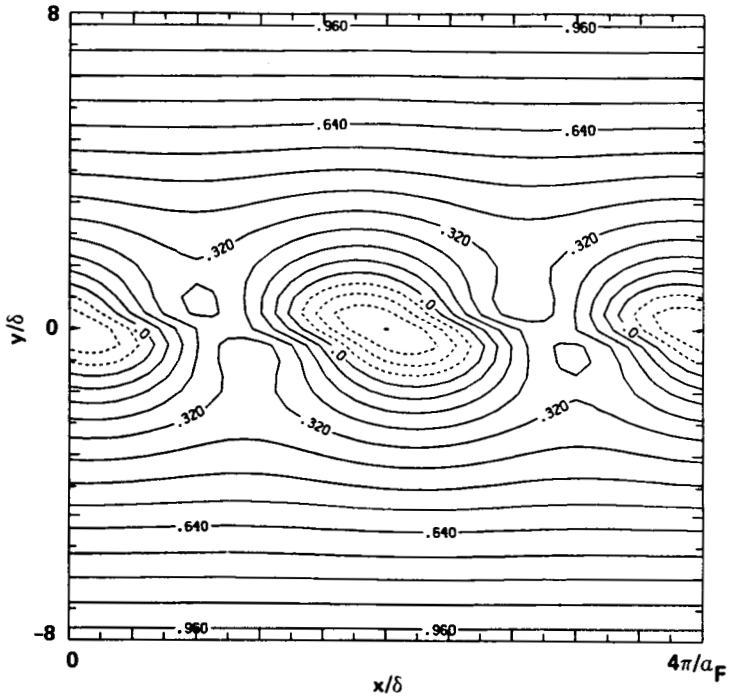

FIGURE 2. Contours of the stream function at time 13 as computed using the amplitude expansion for disturbances which are in-phase.

2.4). What is plotted is an approximation to the energy ($E_{(p,q)}$) in the fundamental and subharmonic modes, as given by;

$$E_{(\alpha_F,0)} = A^2(t) \int_{-\infty}^{\infty} [u^2_{0,(\alpha_F,0)} + v^2_{0,(\alpha_F,0)}]\, dy$$
$$E_{(\alpha_F/2,0)} = B^2(t) \int_{-\infty}^{\infty} [u^2_{0,(\alpha_F/2,0)} + w^2_{0,(\alpha_F/2,0)}]\, dy \qquad (3.1)$$

Note that these are unnormalized energies. The theory is also capable of generating a more complete energy integral, with the total nonlinear form $u_{(\alpha_F,0)}$, rather than the structurally linear form $u_{0,(\alpha_F,0)}$ (see the appendix for an explanation of the notation). This is a matter for future work.

The linear growth of each of the waves (the straight lines on this log-linear graph) is followed by the weak acceleration of the subharmonic (between nondimensional times 13 and 16) due to the effects of the b_1 term. The fundamental then equilibrates due to the action of a_3, while B keeps growing due to the forcing of A, as well as its own ability to extract energy from the mean flow. Once the subharmonic amplitude reaches a critical value, the fundamental is reduced, and the subharmonic equilibrates due to the action of b_4 and a_4. (Note that the final state as predicted here is suspect, since we have discovered that b_4 and a_4 are incomplete as currently calculated. This will be amended in future work.) This graph is representative of

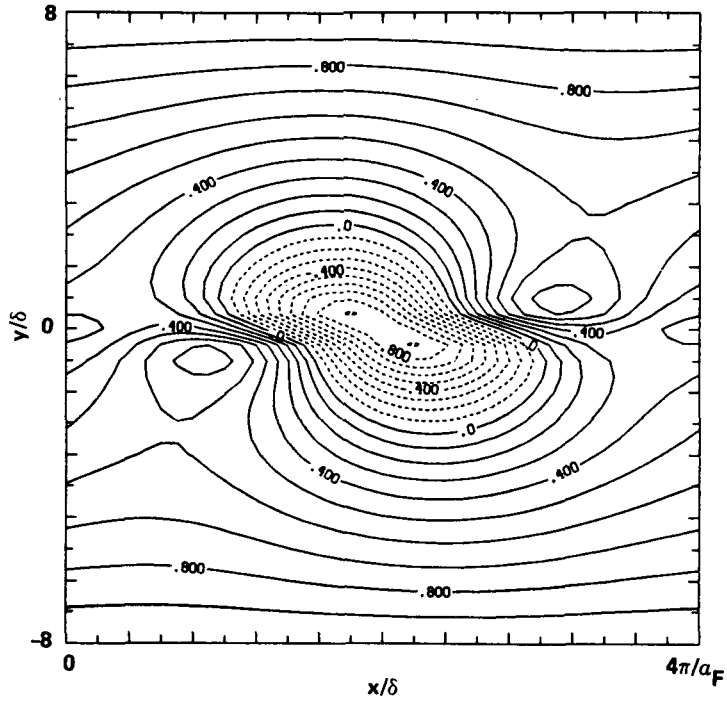

FIGURE 3. Contours of the stream function at time 18 as computed using the amplitude expansion for disturbances which are in-phase.

both the in-phase and out-of-phase calculations, at least qualitatively, and is similar to that in Riley & Metcalfe (1980).

During the linear portion of the evolution, the total stream function field (Figure 2) shows the characteristic scales associated with the fundamental mode, here at time 13 for the in-phase case. The subharmonic is there, with its core at the center of the plot underneath that of the fundamental. However, the subharmonic makes a negligible contribution to the field at this time. The stream function field for the out-of-phase case is the same. Note that this and all the following plots have streamwise domain lengths which equal the wavelength of the subharmonic: therefore, two fundamental vortices and one subharmonic vortex can fit into the domain.

Once the nonlinear interactions become important (nondimensional time of about 18), the flow patterns for the in-phase and out-of-phase cases become different. The total stream function field for the in-phase case (Figure 3) shows an *enhancement* of the original, central, fundamental vortex, at the expense of the vortices to either side, whose torn remnants are at the edge of the graph. This is the 'tearing' mode discussed in Patnaik, Sherman & Corcos (1976). Note that the mixing region, as well as the vortex itself, is smaller here than for the out-of-phase case at the same time (Figure 4). There the subharmonic vortex, made up of two paired, fundamental vortices, fills the graph, showing an increase in the mixing region.

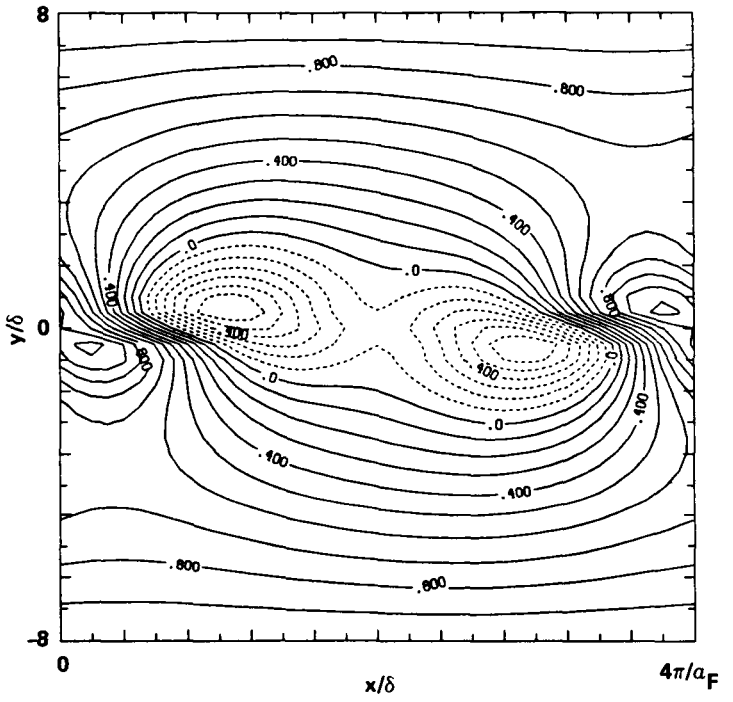

FIGURE 4. Contours of the stream function at time 18 as computed using the amplitude expansion for disturbances which are out-of-phase.

In this application of the amplitude theory, an important experimental and numerical result is reproduced: the effect of the relative phases of the waves. This is an important validation of the approach for this flow which provides encouragement for future applications of the theory. Future applications should include detailed analysis of the role played by each term in the expansion, and should include three-dimensionality as laid out in the appendix. Three-dimensional predictions can be compared to three-dimensional numerical simulations as described in §4 below.

4. Direct numerical simulations

In the numerical simulations, the Navier-Stokes equations (2.2) are solved using a spectral numerical method based on the expansions discussed by Cain, Ferziger & Reynolds (1984). Grid resolutions up to 64^3 were used for the results presented below.

In these preliminary studies, we present results for four different simulations. In the first two cases (Case I and Case II), the fundamental $(\alpha_F, 0)$ as well as the translational mode $(0, \gamma_F)$are initially nonzero. The fundamental mode is taken to be the solution to the Rayleigh equation at $\alpha = \alpha_F$, while the mathematical form

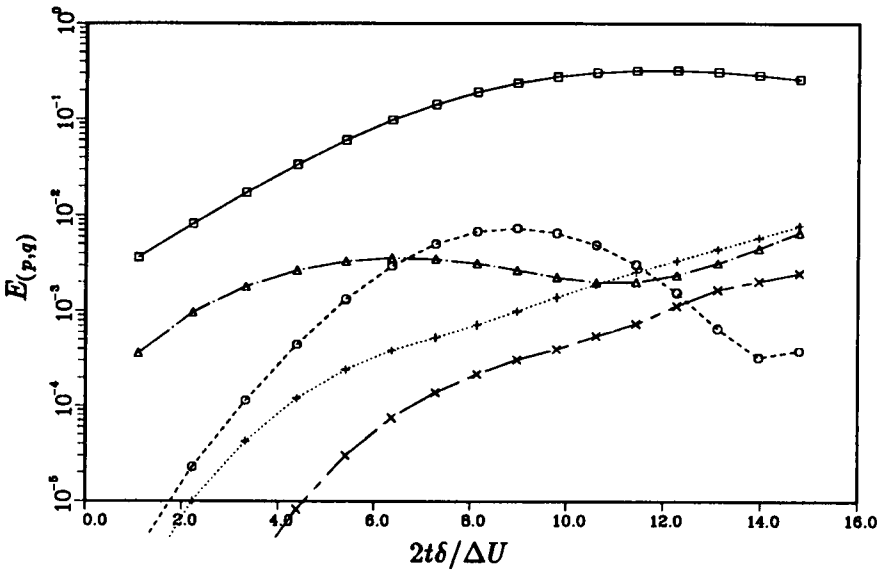

FIGURE 5. Evolution of model energies for CASE I, for the modes: □ , $(\alpha_F, 0)$; ○ , $(2\alpha_F, 0)$; △ , $(0, \gamma_F)$; + (α_F, γ_F); and × $(\alpha_F, 2\gamma_F)$. Modes $(\alpha_F, 0)$ and $(0, \gamma_F)$ were initially excited with energies 2×10^{-3} and 1.5×10^{-4} respectively.

for the translational mode is chosen to be

$$u(x, y, z, 0) = 0,$$
$$v(x, y, z, 0) = Ae^{-2y^2} \cos(\gamma_F z),$$
$$w(x, y, z, 0) = -\frac{4Ay}{\gamma_f} e^{-2y^2} \sin(\gamma_F z).$$

The difference in the two cases is the amplitude A. In Case I it is set to 0.025, while in Case II it is 0.05. In the latter two cases (Case III and Case IV), the fundamental plus the oblique modes (α_F, γ_F) and $(\alpha_F, -\gamma_F)$ are initially nonzero. The normal velocity v for the oblique modes is initially as given above, the other velocity components are such that continuity is satisfied and $\gamma_F u - \alpha_F w = 0$. In Case III the oblique mode is approximately out-of-phase with the fundamental, i. e., it is symmetric about the core of the two-dimensional vortex, while in Case IV the oblique wave is in-phase.

A plot of modal energies versus time for case I is shown in figure 5. In this and in the following, the modal energy is defined by

$$E(\alpha, \gamma, t) = \frac{1}{2} \Sigma_{\alpha,\gamma} \int |\tilde{u}_i(\alpha, y, \gamma, t)|^2 \, dy. \tag{3.2}$$

Here summation over i is implied, and $\tilde{u}_i(\alpha, y, \gamma, t)$ is the Fourier transform of $u_i(x, y, z, t)$ in the (x, z) plane. The summation sign denotes a sum over the modes (α, γ), $(\alpha, -\gamma)$, $(-\alpha, \gamma)$, and $(-\alpha, -\gamma)$.

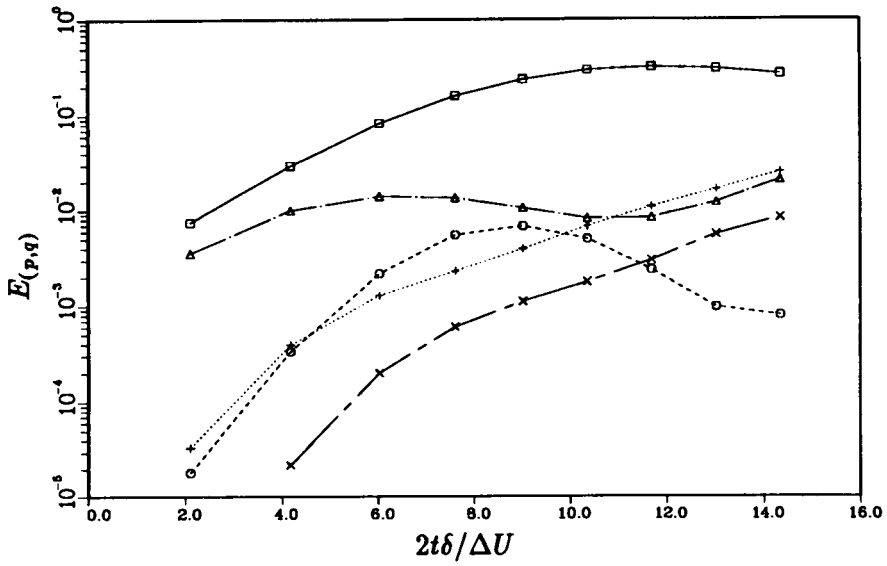

FIGURE 6. Evolution of model energies for CASE II, for the modes: □ , $(\alpha_F, 0)$; ○ , $(2\alpha_F, 0)$; △ , $(0, \gamma_F)$; + (α_F, γ_F); and × $(\alpha_F, 2\gamma_F)$. Modes $(\alpha_F, 0)$ and $(0, \gamma_F)$ were initially excited with energies 2×10^{-3} and 6×10^{-4} respectively.

In Figure 5 we see that the energy in the fundamental mode grows, at first exponentially, then more gradually, and finally levels off at time 12, which corresponds approximately to vortex rollup. At the same time the harmonic $(2\alpha, 0)$ grows very rapidly, peaking at about $t = 9$, and then decays as rollup is completed.

The translative mode, which is only algebraically unstable without the finite amplitude, two-dimensional mode, initially grows very rapidly. Further analysis of the results showed that this growth is initially mainly in the u-component, and is due to the streamwise vortices inducing motion in the y-direction, along the gradient of the mean velocity (Squire mode). As the mixing layer rolls up, vortex stretching occurs along the layer, resulting in further increase in this translative mode. We see that subsequently the oblique mode begins to grow rapidly, and ultimately overtakes the translative mode. Analysis of visualizations (see below) suggests that this growth is due both to the tilting of the streamwise vortices and the distortion of the main spanwise rollers by the the streamwise vortices.

Figure 6 gives the modal energies versus time for Case II, which has the same initial conditions as for Case I except that the translative mode amplitude is increased by a factor of 2. Comparing Figures 5 and 6, we see that the energies in the fundamental mode and its harmonic are essentially the same for the two cases. From an energetics point of view the two-dimensional rollup is totally unaffected by the three-dimensional motions, even though in this latter case the energy in the translative mode is within a factor of two of that in the fundamental mode (at about $t = 2$). Previously Metcalfe *et al.* (1987) observed that, in the interaction of an oblique mode with the fundamental, the fundamental mode played a catalytic

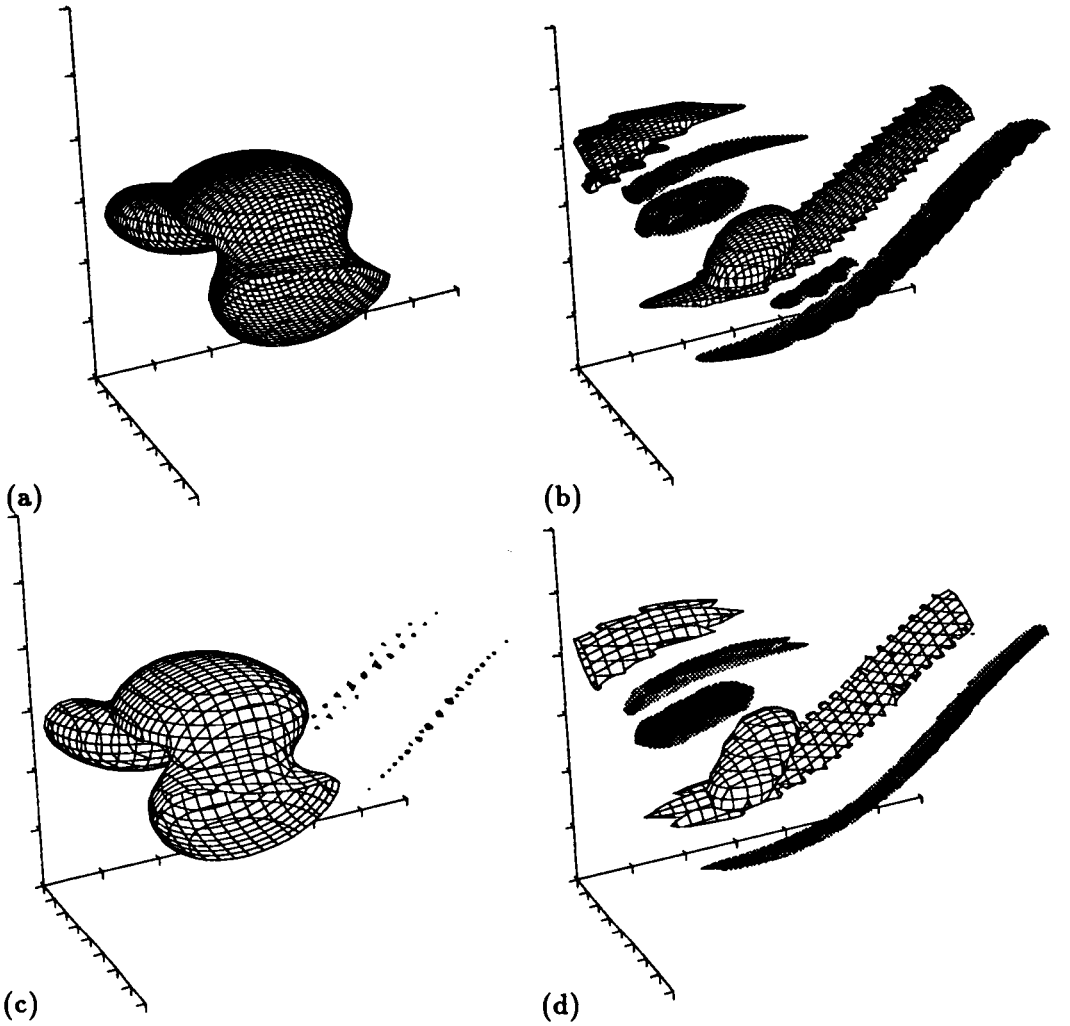

FIGURE 7. Iso-level surfaces of enstrophy *(a,c)* and ω_x *(b,d)* for CASE I *(a,b)* and CASE II *(c,d)*. Solid surfaces represent negative values. Contour levels are 1.5 in *(a,c)*, −0.3 and 0.3 in *(b)* and −0.6 and 0.6 in *(d)*.

role. Its presence was required for the enhanced growth of the oblique mode, but its energy was unchanged by the interaction. The increased energy in the oblique mode came from the mean flow. Our results indicate that this catalytic trait holds for both the fundamental and its harmonic interacting with the translative mode.

The total energy in the three-dimensional modes is significantly different for the two cases. However, examining the results more closely we find that the total energy in a particular three-dimensional mode for Case II is almost exactly four times the corresponding value for Case I. Since the initial amplitude for Case II is exactly twice that for Case I, this is consistent with the interpretation that the development of the three-dimensional dynamics is linear. This result gives some indirect support

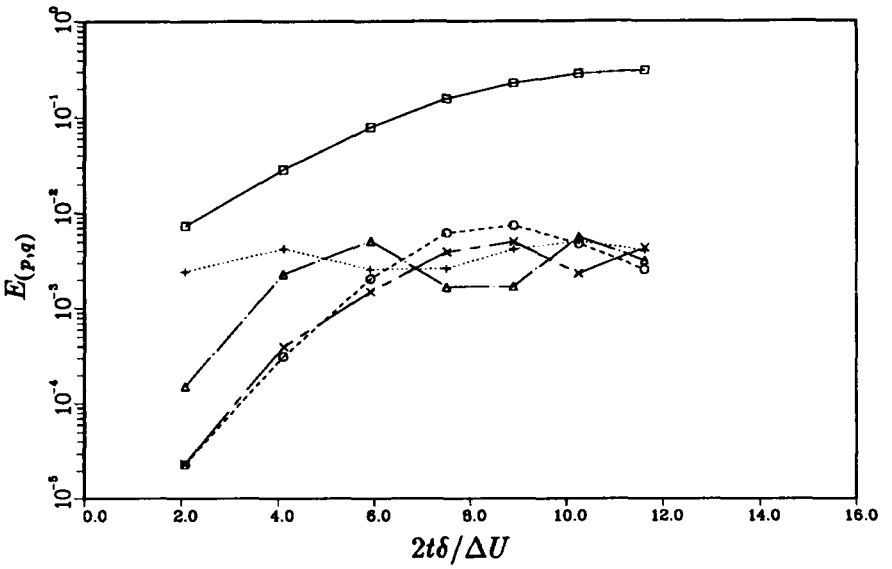

FIGURE 8. Evolution of model energies for CASE III, for the modes: □ , $(\alpha_F, 0)$; ○ , $(2\alpha_F, 0)$; △ , $(0, \gamma_F)$; + (α_F, γ_F); and × $(\alpha_F, 2\gamma_F)$. Modes $(\alpha_F, 0)$ and (α_F, γ_F) were initially excited with energies 2×10^{-3} and 10^{-3} respectively.

to the model of Corcos & Lin (1984) who, although studying the interaction of the fundamental mode with an oblique mode, assumed that the dynamics of the oblique mode were linear.

Perspective plots of iso-value surfaces of both streamwise vorticity (ω_x) and the norm of the vorticity ($\omega = \sqrt{\omega_i \omega_i}$) for these two cases are shown in figure 7. Note that in the plot of ω_x, the contour level for Case II was chosen to be twice that of the level for Case I. We see the development of the streamwise vorticity along the braids, and also these vortices being wrapped into the large-scale vortex core. Note that the streamwise vortices appear to be somewhat flat due to the straining field of the two-dimensional vortices. Also note the appearance of counter-rotating vortices in the core, probably due to the bending of the large-scale vortices by the streamwise vortices. It is interesting to note that the streamwise vorticity plots for the two cases are almost the same, lending strong support to the interpretation that the three-dimensional dynamics are essentially linear. This is surprising in view of the large distortions observed in the flow field. The plots of ω indicate the distortion of the large-scale vortices by the streamwise vortices.

We next discuss the results for the oblique wave cases: Case III, in which the oblique wave disturbance was initially approximately out-of-phase with respect to the vortex core, and Case IV, in which it was in-phase. Plots of the modal energy versus time for Cases III and IV appear in Figures 8 and 9, respectively. First note that in both cases the behavior of the energy in the two-dimensional modes is essentially identical to that for Cases I and II. This is further evidence that the

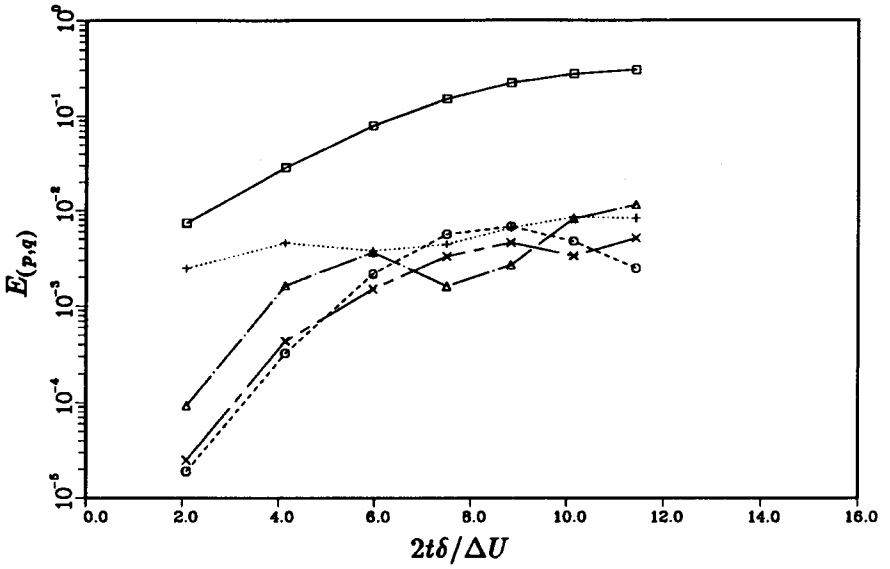

FIGURE 9. Evolution of model energies for CASE I, for the modes: □ , $(\alpha_F, 0)$; ○ , $(2\alpha_F, 0)$; △ , $(0, \gamma_F)$; + (α_F, γ_F); and × $(\alpha_F, 2\gamma_F)$. Modes $(\alpha_F, 0)$ and (α_F, γ_F) were initially excited with energies 2×10^{-3} and 10^{-3} respectively.

two-dimensional modes are unaffected by the three-dimensional motions, and is consistent with the catalytic character of the fundamental mode observed by Metcalfe *et al.* (1987). We further note that in both cases the oblique mode (α_F, γ_F) grows, but not as rapidly as the translational modes in the previous cases. Furthermore, in these cases the translational mode quickly grows from zero to be the same order as the oblique mode.

Though the energetics of the modes are unaffected by the phases, examination of the flow fields reveals that the details of the fields are quite different. Perspective plots of ω_x and ω for both cases appear in Figure 10. The time selected is $t = 10$, when rollup is almost complete. In Case III there is very little evidence of streamwise vorticity in the braid region; it has mainly been rolled into the vortex core. This is due to the fact that, initially, the stagnation point in the braids was near the zero in the streamwise vorticity. In Case IV streamwise vortices are evident, similar to those in Cases I and II. Comparing the plots of ω we see that the flow in the rollup regions is very different for the two cases.

5. Conclusions

From this preliminary study of the sensitivity of the mixing layer to three-dimensional disturbances, we draw a number of tentative conclusions. First it is clear that the mixing layer is sensitive to the wavelength of the disturbances (or frequency in the spatially-developing flow), the relative phases and amplitudes of the disturbances, and to the form of the disturbances. Clearly the disturbance needs to be well-defined in order to predict its behavior.

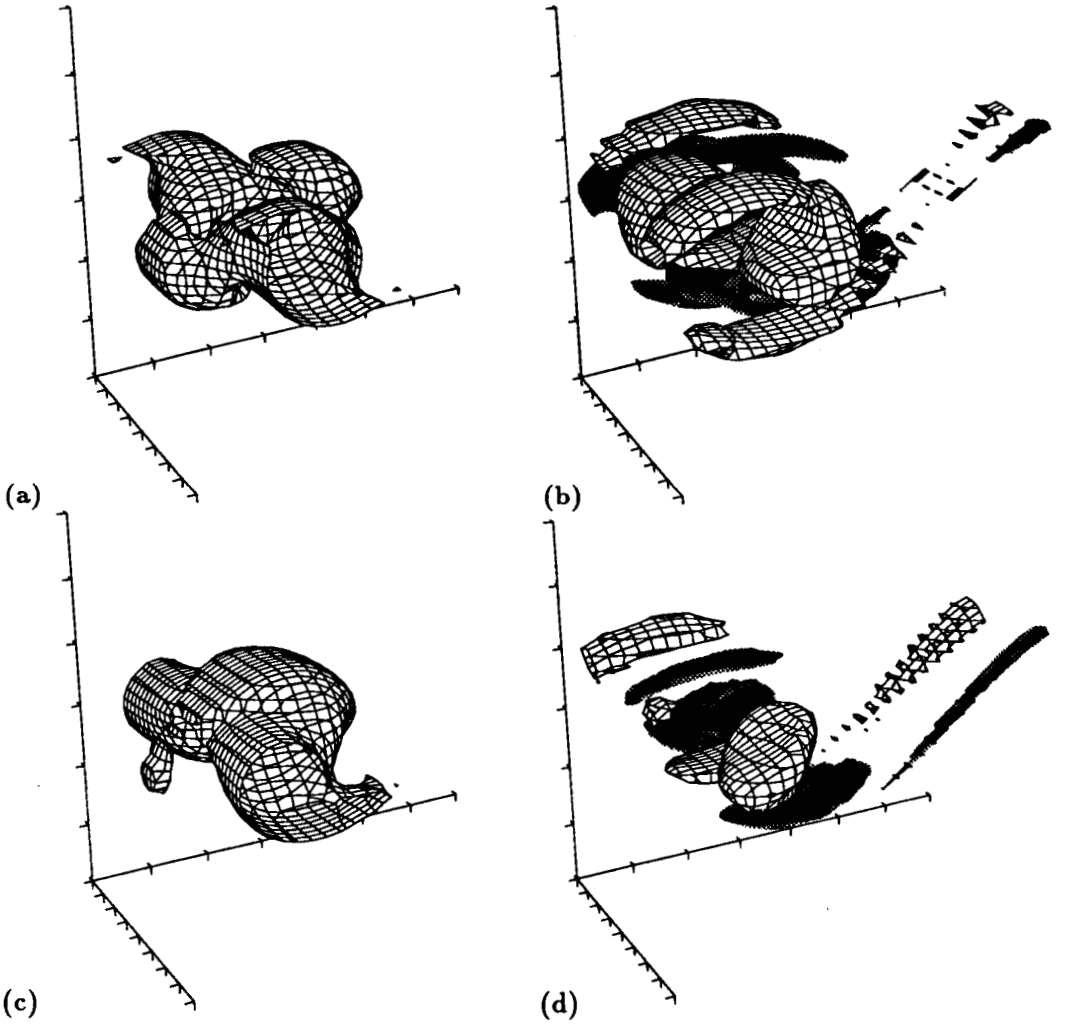

FIGURE 10. Iso-level surfaces of enstrophy *(a,c)* and ω_x *(b,d)* for CASE III *(a,b)* and CASE IV *(c,d)*. Solid surfaces represent negative values. Contour levels are 1.5 in *(a,c)*, −0.25 and 0.25 in *(b)* and −0.5 and 0.5 in *(d)*.

Secondly, it is important to realize that naturally-occurring temporally-evolving mixing layers may develop very different three-dimensional disturbances from those of spatially-evolving mixing layers. The principal initial three-dimensional disturbances in the spatial layer are fairly narrow-banded streamwise vortices, whose development and breakdown appear to be a principal factor in the transition to turbulence of the mixing layer. Their initiation appears to be related to features of the experimental facility. In the temporal layer it is unlikely that this mode is initially excited, and laboratory experiments do not show evidence of these vortices in the braid regions.

Third, at least during vortex rollup, the two-dimensional modes appear to be

almost totally unaffected by the three-dimensional disturbances. In addition, the three-dimensional disturbances behave in an almost linear fashion, being only affected by the two-dimensional rollup and not by their own interactions. This is true even though their energy levels are large, of the order of the energy in the two-dimensional modes.

Fourth, the translative instability appears to be faster growing than that of the oblique modes. This appears to be due to the growth of streamwise velocity fluctuations (the Squire mode). Fifth, the relative phase of the oblique mode perturbation with respect to the fundamental mode is not important in the energetics, but is important in the resulting flow pattern. And sixth, the successful preliminary work with the amplitude expansions suggests that they may be a useful quantitative tool for future research.

Finally, this preliminary study suggests additional simulations and mathematical analysis. For example, it would be useful to more carefully test the amplitude expansion technique by comparing its predictions with the results of direct numerical simulations for cases, both two- and three-dimensional, that treat the exact same initial conditions. If the theory appears to be adequate, then it could be used to better understand the interactions occurring in the simulations, and to determine what combinations of initial conditions might lead to desired features of the mixing layer behavior. With regard to the numerical simulations, there are a large variety of initial conditions which should be explored. Further simulations to determine the range of possible outcomes would be useful.

REFERENCES

BERNAL, L. P. 1981 The coherent structure of turbulent mixing layers. Ph.D. Thesis, California Institute of Technology.

CORCOS, G. M. & LIN, S.-J. 1984 The mixing layer: deterministic models of a turbulent flow. Part 2. The origin of three-dimensional motion. *J. Fluid Mech.* **139**, 67-95.

HERBERT, T. 1983 On perturbation methods in non-linear stability theory. *J. Fluid Mech.* **126**, 167-186.

HO, C.-M. 1988 Private Communication.

HO, C.-M. & HUANG, L.-S. 1982 Subharmonics and vortex merging in mixing layers. *J. Fluid Mech.* **119**, 443-473.

HO, C.-M. & HUERRE, P. 1984 Perturbed free shear layers. *Ann. Rev. Fluid Mech.* **16**, 365-424.

HO, C.-M. & GUTMARK, E. 1987 Vortex induction and mass entrainment in a small-aspect ratio elliptic jet. *J. Fluid Mech.* **179**, 383-405.

HUSAIN, H. S. & HUSSAIN, F. 1986 *Bull. of Am. Phys. Soc.* **31**, 1696.

METCALFE, R. W., ORSZAG, S. A., BRACHET, M. E., MENON, S. & RILEY, J. J. 1987 Secondary instability of a temporally-growing mixing layer. *J. Fluid Mech.* **184**, 207-243.

MICHALKE, A. 1964 On the inviscid instability of the hyperbolic tangent velocity profile. *J. Fluid Mech.* **19**, 543-556.

MONKEWITZ, P. A. 1988 Subharmonic resonance, pairing and shredding in the mixing layer. *J. Fluid Mech.* **188**, 223.

MOURAD, P. D. 1987 A nonlinear wave-wave interaction theory for the generation of multiscale large eddies in the atmospheric boundary layer. Ph.D. Thesis, University of Washington.

MOURAD, P. D. & BROWN R. A. 1988 On multiscale large eddy states in weakly stratified atmospheric boundary layers. submitted to the J. Atmos. Sci.

OSTER, D., & WYGNANSKI I. 1982 The forced mixing layer between parallel streams. *J. Fluid Mech.* **123**, 91-130.

PATNAIK, P. C., SHERMAN, F. S. & CORCOS, G. M. 1976 A numerical simulation of Kelvin-Helmholtz waves of finite amplitude. *J. Fluid Mech.* **73**, 215-240.

PIERREHUMBERT, R. T. & WIDNALL, S. E. 1982 The two- and three-dimensional instabilities of a spatially periodic shear layer. *J. Fluid Mech.* **114**, 59-82.

RILEY, J. J. & METCALFE, R. W. 1980 Direct numerical simulation of a perturbed turbulent mixing layer. *AIAA Paper No. 80-0274.*

THORPE, S. A. 1985 Laboratory observations of secondary structures in Kelvin-Helmholtz billows and consequences for ocean mixing. *Geophys. Astrophys. Fluid Dyn.* **34**, 175-199.

APPENDIX

In this appendix, we develop a theory for wave-wave interactions between oblique waves in supercritical shear flows. A more limited set of theoretical equations based upon the same procedure is used in the body of the text to study the interactions of a fundamental wave and its subharmonic. The more complete equations discussed here were developed during the summer workshop, and will be used in future studies.

The heart of the theory is a set of nonlinear evolution equations which govern the temporal history of the amplitudes of interacting waves. The theory is similar to Stuart's energy integral method, and Lorenz's derivation of his famous amplitude equations for convection. As in these other methods, we manipulate the Navier-Stokes equations in a formal way, without benefit of asymptotic arguments and with severe Fourier, Orr-Sommerfeld and amplitude truncations. Also like them, we hope that these truncations are a good approximation of the full series solution, and that they lend at least a qualitative insight into the physics of the problem. If we had recourse to asymptotically small parameters, a perturbation formalism would determine the relative weights of different physical effects. However, since the flow in question is supercritical, one cannot create a small parameter out of the governing Reynolds number. Neither has the relative energy of the disturbance to the mean flow proven useful as a small parameter. The subsequent evolution of the waves in the presence of the mean flow is governed by the ability of the waves and mean flow to exchange energy with each other, which, even in an initially linear regime, is independent of this parameter. With these obvious choices removed for supercritical flows there are no readily apparent small parameters that we can use. Supercritical flows generally evolve quickly away from any given initial state to a relatively remote state – a process which is not usually amenable to asymptotic analysis. With the formalism developed here, we can build tools which are simpler to use than the full Navier-Stokes equations, as well as lay bare the underlying physical processes. It becomes a powerful tool of analysis when used in tandem with experimental observations and/or direct numerical simulations.

The theory starts with the fully nonlinear, nondimensional Navier-Stokes equations, in the coordinate system used in the text. Separate the mean flow (a function of y and t alone) from the wavelike part (oscillatory in x and z) of the dependent variables, with the following notation:

$$\mathbf{U}(x,y,z,t) = \mathbf{U}_0(y) + \overline{\mathbf{U}}(y,t) + \mathbf{u}(x,y,z,t) \tag{A1.1}$$

$$P = \overline{P}(y,t) + p(x,y,z,t) \tag{A1.2}$$

The vector $\mathbf{U}_0 \equiv (U_0, 0, 0)$ defines the original flow field which will house the interacting waves. We have chosen:

$$U_0 \equiv \mathrm{erf}(\sqrt{\pi}y) \tag{A1.3}$$

where y is nondimensionalized by the initial vorticity thickness δ. This profile is selected because it is the self-similar laminar profile for a temporally-evolving mixing

layer. The mean pressure field will remain unspecified, as it does not enter into the problem. The vector $\overline{\mathbf{U}} \equiv (\overline{U}, 0, \overline{W})$ represents a time-dependent modification to the initial mean flow caused by nonlinear feedback from the spatially oscillating part of the field. It is calculated as part of the solution, as well as the modified mean pressure, given by $\overline{P}$.

Substituting the expansion (A1) into the Navier-Stokes equations one obtains the following:

$$u_t + U_0 u_x + v\frac{\partial}{\partial y}U_0 - \frac{1}{Re}\Delta u + p_x = -(\mathbf{u} + \overline{\mathbf{U}}) \cdot \nabla(u + \overline{U}) + \overline{\mathbf{u} \cdot \nabla u} \quad (A2.1)$$

$$v_t + U_0 v_x - \frac{1}{Re}\Delta v + p_y = -(\mathbf{u} + \overline{\mathbf{U}}) \cdot \nabla(v) + \overline{\mathbf{u} \cdot \nabla v} \quad (A2.2)$$

$$w_t + U_0 w_x - \frac{1}{Re}\Delta w + p_z = -(\mathbf{u} + \overline{\mathbf{U}}) \cdot \nabla(w + \overline{W}) + \overline{\mathbf{u} \cdot \nabla w} \quad (A2.3)$$

$$\overline{U}_t - \frac{1}{Re}\overline{U}_{yy} = -\overline{\mathbf{u} \cdot \nabla u} \quad (A2.4)$$

$$\overline{W}_t - \frac{1}{Re}\overline{W}_{yy} = -\overline{\mathbf{u} \cdot \nabla w} \quad (A2.5)$$

with:

$$\Delta \equiv \frac{\partial^2}{\partial x^2} + \frac{\partial^2}{\partial y^2} + \frac{\partial^2}{\partial z^2},$$

and the bar over the non-linear terms indicates the average in x and z (but not time) of each term.

A.1 Fourier expansions

The next step is to write the spatially oscillating components of the flow in a highly-truncated Fourier series in x and z. This series is truncated at the beginning so that the smallest number of Fourier components need be considered.

The collective nonlinear behavior of the primary waves with wavenumber vectors $(\alpha, 0)$, $(\alpha/2, 0)$, $(\alpha/2, \gamma)$ and (α, γ) is the main focus of this study. (Note that, for notational simplicity in this Appendix, we are dropping the subscript F, which denotes the fundamental mode in the main body of this paper.) This theory describes the evolution of a flow field by studying components of the Fourier transform of the velocity fields. The choice of the primary waves is motivated by the *observation* that these are significant waves: with this theory we will only attempt to explain their behavior, and can only suggest why these should be the waves of choice. According to linear theory, $(\alpha, 0)$ (also called the fundamental mode) initially grows most quickly, and $(\alpha/2, 0)$ is its subharmonic. The subharmonic is significant because after the roll-up of the initial vortices (equilibration of the fundamental wave), the subharmonic is observed to grow resulting in the pairing of the two-dimensional vortices. The pairing process is dependent upon the relative phases of $(\alpha, 0)$ and $(\alpha/2, 0)$, among other things. Observations show that the pairing is followed by, and sometimes concurrent with, the development of three-dimensionality in the

originally two-dimensional flow. Spectrally, this is represented by the inclusion of oblique waves (α,γ) and $(\alpha/2,\gamma)$.

Other waves could also be chosen as primary: for example, an interesting choice is the wavenumber vector $(0,\gamma)$, which denotes a system of longitudinal vortices. The formalism would proceed in the same fashion if these were included, with different evolution equations as the result. However, since this is as yet only a temporal theory, and $(0,\gamma)$ seems to be more relevant for spatially developing flow fields, we ignore this mode for now.

There is another class of waves which are included here, because they are forced by various combinations of the primary waves and their complex conjugates. For short times, these waves are observed to be slaved to the primary ones, that is the dynamics of these modes are dominated by the forcing. Their intrinsic dynamics are considered insignificant so no extra degrees of freedom will be required to account for their effects. For this limited study, we only include the first harmonic of $(\alpha,0)$, given by wavenumber vector $(2\alpha,0)$ because it is important for the interaction between $(\alpha,0)$ and (α,γ). We also assume that the modification to the mean and the so called Squire modes (see below) remain slaved to the primary waves.

Which waves to include, and whether they are included as free or forced waves, are subtle, contentious, important and open questions. They represent large areas of possible improvement as well as additional complexity.

Finally note that while we have only been discussing modes of the form (p,q), with p and q positive, all the modes $(\pm p,\pm q)$ are important. However, the velocity fields are real, which implies that two of these modes are not independent due to conjugate symmetry. In addition, we will require that the velocity be mirror symmetric in the z direction, which will eliminate the independence of another mode. This is a symmetry which is preserved by the Navier-Stokes equations so that with an initial condition satisfying this symmetry the solution will remain symmetric. Thus with the reality of the velocity and the mirror symmetry, only the modes (p,q) with p and q positive are independent.

For each Fourier mode (p,q) the y-dependence of the three velocity components must be represented. However, the constraint of continuity eliminates a degree of freedom so that only two y functions need be considered. To do this we define two new functions of y:

$$\psi \equiv \frac{i\hat{v}}{\delta}; \qquad \omega \equiv p\hat{w} - q\hat{u}, \tag{A3}$$

where $\hat{u}$, $\hat{v}$ and $\hat{w}$ represent the Fourier coefficients of the velocity components for the given wave number and $\delta = \sqrt{p^2+q^2}$. This notation is chosen because ψ can be interpreted as a stream function and ω is proportional to the y component of the vorticity; ω is also referred to as the Squire mode. Given ψ and ω for a particular Fourier mode, the velocity components can be recovered as follows:

$$\hat{u} = \frac{\delta p\frac{\partial\psi}{\partial y} - q\omega}{\delta^2}; \qquad \hat{v} = -i\delta\psi; \qquad \hat{w} = \frac{\delta q\frac{\partial\psi}{\partial y} + p\omega}{\delta^2}. \tag{A4}$$

The equations for ψ and ω for our Fourier mode (p,q) can easily be derived from the Navier-Stokes equations, with the result;

$$\left[\frac{\partial}{\partial t}+ipU_0\right]\hat{\Delta}\psi - ip\psi\frac{d^2U_0}{dy^2} - \frac{1}{\mathrm{Re}}\hat{\Delta}^2\psi = \frac{i}{\delta}\left[\frac{\partial(ip\Gamma_x+iq\Gamma_z)}{\partial y}+\delta^2\Gamma_y\right]_{(p,q)} \quad (A5.1)$$

$$\left[\frac{\partial}{\partial t}+ipU_0\right]\omega - i\delta q\psi\frac{dU_0}{dy} - \frac{1}{Re}\nabla^2\omega = [q\Gamma_x - p\Gamma_z]_{(p,q)}\,; \quad (A5.2)$$

where, $\Gamma = (\overline{\mathbf{U}}+\mathbf{u})\cdot\nabla(\overline{\mathbf{U}}+\mathbf{u})$, the subscript on Γ refers to the vector component, $\hat{\Delta}$ is the Fourier transformed Laplacian ($\hat{\Delta} = \partial^2/\partial y^2 - p^2 - q^2$) and $\delta^2 = p^2+q^2$. The notation $[\cdot]_{(p,q)}$ indicates the (p,q) Fourier mode of the quantity in brackets. The above equations are valid for all wave number pairs except $(0,0)$. The Fourier transformed Navier-Stokes equations for $\overline{U}$ and $\overline{W}$ are used directly for this mode.

We now introduce real amplitudes $A(t)$, $B(t)$, $C(t)$, $D(t)$ and phase functions $\theta_A(t)$, $\theta_B(t)$, $\theta_C(t)$, $\theta_D(t)$, one for each of the primary waves. The ultimate goal is to derive ordinary differential equations which govern the evolution of these functions. The forced first harmonic of $(\alpha,0)$, the forced modifications to the mean flow due to the various waves and the Squire modes do not have independent amplitudes. Rather, they are functions of the amplitudes of the forcing waves. This is consistent with the equations, and is as described in Herbert (1983). The expansion for u is given below. Those for v and w are similar in form. Note that the Fourier mode $(2\alpha,0)$ is especially busy, with two contributions. The functions $\hat{u}_{A,(2\alpha,0)}$ and $\hat{u}_{C,(2\alpha,0)}$ represent the response of the $(2\alpha,0)$ mode to forcing by the $(\alpha,0)$ mode and (α,γ) mode respectively.

$$\begin{aligned}
u(x,y,z,t) = 2\mathrm{Real}\Big\{ & A(t)\hat{u}_{(\alpha,0)}e^{i(\alpha x-\theta_A(t))} + B(t)\hat{u}_{(\alpha/2,0)}e^{i(\alpha x/2-\theta_B(t))} \\
& + \left[A^2(t)\hat{u}_{A,(2\alpha,0)}e^{-2i\theta_A(t)} + C^2(t)\hat{u}_{C,(2\alpha,0)}e^{-2i\theta_C(t)}\right]e^{2i\alpha x}\Big\} \\
& + 4C(t)\mathrm{Real}\left\{\hat{u}_{(\alpha,\gamma)}e^{i(\alpha x-\theta_C(t))}\right\}\cos(\gamma z) \\
& + 4D(t)\mathrm{Real}\left\{\hat{u}_{(\alpha/2,\gamma)}e^{i(\alpha x/2-\theta_D(t))}\right\}\cos(\gamma z) \\
& + A^2(t)\overline{U}_A + B^2(t)\overline{U}_B + C^2(t)\overline{U}_C + D^2(t)\overline{U}_D,
\end{aligned} \quad (A6)$$

where the dependence of $\hat{u}$ and $\overline{U}$ on y and t is understood.

A.2 Streamfunction equations

By substituting expansions like (A6) into the Navier-Stokes equations and converting to ψ and ω as in (A5) we can write the truncated modal equations governing each Fourier mode. In writing these equations we will make use of the following operators:

$$M_{(p,q)} \equiv \frac{\partial^2}{\partial y^2} - (p^2+q^2) \quad (A7.1)$$

$$L_{(p,q)} \equiv i(p^2+q^2)^{1/2}U_0 M_{(p,q)} - i(p^2+q^2)^{1/2}\frac{\partial^2 U_0}{\partial y^2} - \frac{1}{Re}M^2_{(p,q)} \tag{A7.2}$$

$$\Omega(\psi_{(p,q)},\psi_{(\pi,\rho)}) \equiv ip\left[\psi_{(p,q)}\frac{\partial}{\partial y}M_{(\pi,\rho)}\psi_{(\pi,\rho)} - \left(\frac{\partial}{\partial y}\psi_{(\pi,\rho)}\right)M_{(p,q)}\psi_{(p,q)}\right] \tag{A7.3}$$

$$N(p,q;\pi,\rho) \equiv i(p+\pi)\left(i\pi\hat{u}_{(p,q)}\hat{w}_{(\pi,\rho)} + \hat{v}_{(p,q)}\frac{\partial}{\partial y}\hat{w}_{(\pi,\rho)} + i\rho\hat{w}_{(p,q)}\hat{w}_{(\pi,\rho)}\right) - \frac{\partial}{\partial y}\left(i\pi\hat{u}_{(p,q)}\hat{u}_{(\pi,\rho)} + \hat{v}_{(p,q)}\frac{\partial}{\partial y}\hat{u}_{(\pi,\rho)} + i\rho\hat{w}_{(p,q)}\hat{u}_{(\pi,\rho)}\right) \tag{A7.4}$$

Below are examples of the resulting equations governing the stream-functions ψ. Equations for the Squire modes ω are similar. Note that the non-linear terms are expressed (using the above operators) in terms of the stream function whenever possible, but that the terms involving the N operator require the velocity components, which are found using (A4). Also note that these are partial differential equations in y and t. First is the equation for the stream function of the fundamental wave.

$$\begin{aligned}\left(\frac{\partial}{\partial t}+a(t)\right)M_{(\alpha,0)}\psi_{(\alpha,0)} + L_{(\alpha,0)}\psi_{(\alpha,0)} &= \frac{B^2}{A}e^{-i(2\theta_B-\theta_A)}\Omega(\psi_{(\alpha/2,0)},\ \psi_{(\alpha/2,0)}) \\ &+ \frac{D^2}{A}e^{-i(2\theta_D-\theta_A)}\left[N(\alpha/2,\gamma;\alpha/2,-\gamma)+N(\alpha/2,-\gamma;\alpha/2,\gamma)\right] \\ &+ A^2\left[\left\{\Omega(\psi^*_{(\alpha,0)},\psi_{A,(2\alpha,0)})+\Omega(\psi_{A,(2\alpha,0)},\psi^*_{(\alpha,0)})\right\}+\Omega(\psi_{(\alpha,0)},\psi_{A,(0,0)})\right] \\ &+ C^2\left[\left\{\Omega(\psi^*_{(\alpha,0)},\psi_{C,(2\alpha,0)})+\Omega(\psi_{C,(2\alpha,0)},\psi^*_{(\alpha,0)})\right\}+\Omega(\psi_{(\alpha,0)},\psi_{C,(0,0)})\right] \\ &+ \left[B^2\Omega(\psi_{(\alpha,0)},\psi_{B,(0,0)})+D^2\Omega(\psi_{(\alpha,0)},\psi_{D,(0,0)})\right].\end{aligned} \tag{A8.1}$$

Where $\psi_{(0,0)} = \int \overline{U}(y')\,dy'$ and the subscript letter on $\psi_{(0,0)}$ and $\psi_{(2\alpha,0)}$ indicate which primary mode is providing the forcing. The five different terms on the right-hand side of (A8.1) represent the following effects on the fundamental (in order): 1) the effects of the subharmonic 2) the influence of the oblique subharmonic, 3) the combined influence of those parts of the forced first harmonic and the modification of the mean flow which are caused by the fundamental wave, 4) the combined influence of those parts of the first harmonic and the modification of the mean flow which are forced by (α,γ), and 5) the influence of those modifications to the mean flow which are induced by the other waves. Next are the equations for the two parts of the forced first harmonic,

$$\left(\frac{\partial}{\partial t}+2a(t)\right)M_{(2\alpha,0)}\psi_{A,(2\alpha,0)} + L_{(2\alpha,0)}\psi_{A,(2\alpha,0)} = \Omega(\psi_{(\alpha,0)},\psi_{(\alpha,0)}) \tag{A8.2}$$

$$\left(\frac{\partial}{\partial t}+2c(t)\right)M_{(2\alpha,0)}\psi_{C,(2\alpha,0)} + L_{(2\alpha,0)}\psi_{C,(2\alpha,0)} = N(\alpha,\gamma;\alpha,-\gamma)+N(\alpha,-\gamma;\alpha,\gamma) \tag{A8.3}$$

The first equation (A8.2) describes the part forced by the fundamental $(\alpha, 0)$, while the second equation (A8.3) describes the part forced by the oblique fundamental (α, γ). Finally, we present the equation for the modification of the mean flow by the fundamental mode.

$$\left(\frac{\partial}{\partial t} + \frac{2}{A}\frac{\partial A}{\partial t}\right)\frac{\partial^2}{\partial y^2}\overline{U}_A + L_{(0,0)}\overline{U}_A = \frac{\partial}{\partial y}\left[\Omega(\psi_{(\alpha,0)}, \psi^*_{(\alpha,0)}) + \Omega(\psi^*_{(\alpha,0)}, \psi_{(\alpha,0)})\right] \tag{A8.4}$$

For equations (A8.2,A8.3 and A8.4) we are only interested in particular solutions since these are modes which are slaved to the primary modes. Equations for modes not presented above and equations for ω have similar form.

Functions a, b, c and d which appear in the above equations are defined below. They are the left-hand sides of what will become coupled Landau equations, which will give temporal development of the amplitudes and phases of the disturbances.

$$a(t) \equiv \frac{1}{A}\frac{dA}{dt} - i\frac{d}{dt}\theta_A \tag{A9.1}$$

$$b(t) \equiv \frac{1}{B}\frac{dB}{dt} - i\frac{d}{dt}\theta_B \tag{A9.2}$$

$$c(t) \equiv \frac{1}{C}\frac{dC}{dt} - i\frac{d}{dt}\theta_C \tag{A9.3}$$

$$d(t) \equiv \frac{1}{D}\frac{dD}{dt} - i\frac{d}{dt}\theta_D \tag{A9.4}$$

A.2 The amplitude expansion

The next step in the development of the theory is to develop expansions to describe the time and y dependence of the ψ's and the time dependence of the functions a, b, c and d. In choosing these expansions we arrange the terms so that the dependence on the amplitude and phase functions A, B, C, D, θ_A, θ_B, θ_C and θ_D, of the left and right hand sides of equations like (A8.1) will match. Thus the expansion for $\psi_{(\alpha,0)}$ is

$$\begin{aligned}\psi_{(\alpha,0)}(y,t) = {} & \phi_{0,(\alpha,0)} + \phi_{1,(\alpha,0)}\frac{B^2}{A}e^{-i(2\theta_B-\theta_A)} + \phi_{2,(\alpha,0)}\frac{D^2}{A}e^{-i(2\theta_D-\theta_A)} \\ & + \left[A^2\phi_{3,(\alpha,0)} + B^2\phi_{4,(\alpha,0)} + C^2\phi_{5,(\alpha,0)} + D^2\phi_{6,(\alpha,0)}\right] \\ & + \frac{BCD}{A}\left[\phi_{7,(\alpha,0)}e^{i(\theta_A-\theta_B-\theta_C+\theta_D)} + \phi_{8,(\alpha,0)}e^{i(\theta_A+\theta_B-\theta_C+\theta_D)}\right. \\ & \left. + \phi_{9,(\alpha,0)}e^{i(\theta_A-3\theta_B-\theta_C+\theta_D)}\right] + \ldots,\end{aligned} \tag{A11}$$

where it is understood that the ϕ_j are functions of y. Note that the amplitude and phase dependence of the first several terms is the same as the coefficients appearing on the right hand side of (A8.1). In addition there are the terms with coefficient

BCD/A, these terms arise because of the time derivative operator on the left side of (A8.1), that is the term

$$\left(\frac{\partial}{\partial t} + a(t)\right) M_{(p,q)}\psi_{(p,q)}.$$

If we had used the 'shape' assumption of Stuart or Lorenz, (A11.1) would consist of only the first term in this expansion, which is the solution to the Orr-Sommerfeld equation (see below). The current expansions retain more of the relevant physical processes. Similarly we obtain expansions for the time functions which have amplitude and phase dependencies dictated by the form of the equations like (A8.1). For example compare (A11) above with (A12.1) below. In the following equations the coefficients a_i, b_i, c_i, and d_i (Landau constants) are complex constants.

$$\begin{aligned} a(t) = a_0 &+ a_1\frac{B^2}{A}e^{-i(2\theta_B-\theta_A)} + a_2\frac{D^2}{A}e^{-i(2\theta_D-\theta_A)} + \left[a_3A^2 + a_4B^2 + a_5C^2 + a_6D^2\right] \\ &+ \frac{BCD}{A}\left[a_7e^{i(\theta_A-\theta_B-\theta_C+\theta_D)} + a_8e^{i(\theta_A+\theta_B-\theta_C+\theta_D)}\right. \\ &\left. + a_9e^{i(\theta_A-3\theta_B-\theta_C+\theta_D)}\right] + \ldots \end{aligned} \tag{A12.1}$$

$$\begin{aligned} b(t) = b_0 &+ b_1Ae^{-i(\theta_A-2\theta_B)} + b_2\frac{CD}{B}e^{-i(\theta_C-\theta_D-\theta_B)} + \left[b_3A^2 + b_4B^2 + b_5C^2 + b_6D^2\right] \\ &+ b_7A^2e^{-2i(\theta_A-2\theta_B)} + b_8D^2e^{-2i(\theta_D-\theta_B)} \\ &+ A^2e^{-i(\theta_A-2\theta_B)}\left[b_9\cos(\theta_A-2\theta_B) + b_{10}\sin(\theta_A-2\theta_B)\right] \\ &+ \frac{ACD}{B}\left[b_{11}e^{-i(\theta_A-3\theta_B+\theta_C-\theta_D)} + b_{12}e^{i(\theta_A+\theta_B-\theta_C-\theta_D)}\right. \\ &+ b_{13}e^{-i(\theta_A-\theta_B-\theta_C+\theta_D)} + e^{-i(\theta_A-2\theta_B)}\left\{b_{14}\cos(\theta_B-\theta_C+\theta_D)\right. \\ &\left.\left. + b_{15}\sin(\theta_B-\theta_C+\theta_D)\right\}\right] + \ldots \end{aligned} \tag{A12.2}$$

$$\begin{aligned} c(t) = c_0 &+ c_1A^2e^{-2i(\theta_A-\theta_B)} + c_2\frac{BD}{C}e^{-i(\theta_B+\theta_D-\theta_C)} + \left[c_3A^2 + c_4B^2 + c_5C^2 + c_6D^2\right] \\ &+ \frac{ABD}{C}\left[c_7e^{-i(\theta_A-\theta_B-\theta_C+\theta_D)} + c_8e^{-i(\theta_A+\theta_B-\theta_C-\theta_D)}\right] + \ldots \end{aligned} \tag{A12.3}$$

$$\begin{aligned} d(t) = d_0 &+ d_1Ae^{-i(\theta_A-2\theta_D)} + d_2\frac{BC}{D}e^{-i(\theta_C-\theta_B-\theta_D)} + \left[d_3A^2 + d_4B^2 + d_5C^2 + d_6D^2\right] \\ &+ d_7A^2e^{-2i(\theta_A-2\theta_D)} + d_8B^2e^{-2i(\theta_B-\theta_D)} + d_9\frac{ACD}{B}e^{-i(\theta_A-3\theta_B+\theta_C-\theta_D)} \\ &+ \frac{ABC}{D}\left[d_{10}e^{-i(\theta_A-\theta_B+\theta_C-3\theta_D)} + d_{11}e^{i(\theta_A-\theta_B-\theta_C+\theta_D)}\right. \\ &\left. + d_{12}e^{-i(\theta_A+\theta_B-\theta_C-\theta_D)}\right] + \ldots \end{aligned} \tag{A12.4}$$

Combining equations (A9) and (A12), ordinary differential equations for the amplitude and phase functions are obtained. It is these evolution equations that must be solved to obtain the time dependence of the desired solution. All that remains

is to compute the evolution coefficients a_i etc. The methodology for computing them is discussed below; however, they have not yet been computed for this three-dimensional case. Still, we can make some qualitative inferences from the form of these equations. Consider (12), in the form of $Aa(t)$, $Bb(t)$, etc., so that one can consider $dA/dt\ldots$ If $A(0) \neq 0$ while $B(0)$, $C(0)$, $D(0) = 0$, only the fundamental mode will evolve, since the other modes will remain zero. Their initially zero growth rate ($dB/dt(t = 0) = 0$, etc.) will remain zero ($dB/dt = 0$, etc. $\forall t$). Eventually, the fundamental will equilibrate due to the feedback from the modification to the mean flow and forced first harmonic, embodied in $a_3 A^3$. This agrees with observations and the numerical simulations of Metcalfe, *et al.* (1988) among others. If only the fundamental and subharmonic have nonzero initial amplitudes, they will interact, causing pairing; however, the three-dimensional modes will remain zero, again because their forcing requires that at least one of them be nonzero in the initial conditions to get a nonzero time rate of change. Consider the case of nonzero initial amplitudes, save for the oblique subharmonic $(\alpha/2, \gamma)$. The fundamental and subharmonic will interact as before, while the more slowly growing, or even decaying oblique fundamental (α, γ) is initially of little consequence. The oblique subharmonic will remain negligible, because it requires the combined effort of the two-dimensional subharmonic and oblique fundamental to stimulate it into growth, represented mathematically by the d_2 term in (A12.4). When the fundamental gets large enough, its forced first harmonic will stimulate the oblique fundamental into accelerated growth (represented mathematically by the c_1 term in (A12.3)). This should occur at least simultaneously with, if not after pairing, because the a_1 and b_1 expressions which govern pairing are larger than the c_1 term, assuming comparable sizes of these coefficients. Finally, after the oblique fundamental mode reaches a size of some consequence, the oblique subharmonic will appear, driven by the two-dimensional subharmonic and the oblique fundamental via at least the d_2 term. It is too difficult to judge what happens beyond this. This scenario, suggested by the equations, is similar to numerical simulations and observations. Actual integration of the evolution equations is required to verify these conjectures.

One can test the individual effects and hence the importance of each of these terms through a series of integrations of the equations with and without the expression of interest. This will allow the analysis of the roles played by the various interactions. Comparisons with Corcos and Lin (1984) would be interesting, since they considered a partially linearized form of the Navier-Stokes equations, which contain, some, but not all of the interactions built into our equations. Future work will consider such a program of experimental mathematics.

Evaluating the expansion coefficients

Substituting expansions like (A11) and (A12) in (A8) and equating like terms in the amplitude and phase functions results in a series of linear equations for the expansion functions ϕ_i. The equations for ϕ_0 are Orr-Sommerfeld equations. For example, the $(\alpha, 0)$ equation is

$$a_0 M_{(\alpha,0)} \phi_{0,(\alpha,0)} + L_{(\alpha,0)} \phi_{0,(\alpha,0)} = 0, \qquad (A13.1)$$

where a_0 is the Orr-Sommerfeld eigenvalue and ϕ_0 is the eigenfunction. We will take as the solution the first (most unstable) eigenfunction and eigenvalue. The rest of the equations are linear, inhomogeneous and of the form

$$(\eta_j + a_0)M_{(\alpha,0)}\phi_{j,(\alpha,0)} + L_{(\alpha,0)}\phi_{j,(\alpha,0)} = Y_j - a_j M_{(\alpha,0)}\phi_{0,(\alpha,0)}, \qquad (A13.2)$$

where the η_j are nonzero complex numbers, and the Y_j are functions of y. Both η_j and Y_j can be determined from the solutions already obtained for a_i, b_i etc. and ϕ_i for $i < j$. As an example, the remainder of the analysis will be done for the fundamental mode $(\alpha, 0)$; the analysis for the other modes is similar.

Since the functions ψ are only defined to within a multiplicative constant, a normalization condition is necessary to obtain a solution to these equations. Also, since the linear solution $\phi_{0,(\alpha,0)}(y)$ has an arbitrary magnitude, so will the corrections (ϕ_j). It is convenient to choose a linear norm, and apply it in a way which allows the determination of the Landau coefficients. Herbert (1983) chooses a linear normalization, (designated by $\{\cdot\}$), such that the following normalization condition is satisfied:

$$\{\psi_{(\alpha,0)}(y,t)\} = 1 \quad \text{for all time.}$$

We use $\{\psi_{(\alpha,0)}(y,t)\} = \int_{-\infty}^{\infty} \psi_{(\alpha,0)}(y,t)dy$, although any linear norm which is not zero for ψ and ϕ_0 would do. Note that this condition is not simply $\{\phi_{0,(\alpha,0)}\} = 1$. This unusual choice of normalization places conditions on all of the $\phi_{n,(\alpha,0)}$, namely:

$$\{\psi_{(\alpha,0)}(y,t)\} = \left\{\sum_{n=0}^{\infty} F_n(t)\phi_{n,(\alpha,0)}(y)\right\} = \sum_{n=0}^{\infty} F_n(t)\left\{\phi_{n,(\alpha,0)}(y)\right\} = 1 \qquad (A14)$$

Since the $F_n(t)$ are functions of time (dependent on the amplitude and phase functions, see equation A11) and $F_0 = 1$, this condition is satisfied by requiring

$$\{\phi_{j,(\alpha,0)}\} = \begin{cases} 1, & j = 0; \\ 0, & j > 0. \end{cases} \qquad A15$$

Setting the right side of (A13.2) to zero produces the Orr-Sommerfeld equation with a parameter different from the first eigenvalue ($\eta_j \neq 0$); therefore, equation (A13.2) does not have homogeneous solutions (unless $\eta_j + a_0$ happens to also be an eigenvalue). The solution to (A13.2) is therefore just the sum of the responses to the individual inhomogeneous terms:

$$\phi_{j,(\alpha,0)} = \Upsilon_j - \frac{a_j}{\eta_j}\phi_{0,(\alpha,0)}, \qquad (A16)$$

where Υ_j is the solution to Equation (A13) corresponding to Y_j, and $a_j/\eta_j\phi_{0,(\alpha,0)}$ is the solution corresponding to the ϕ_0 term on the right side of (A13.2). Applying the normalization condition to (A16) and using (A15) the value for the Landau constant a_j is obtained,

$$a_j = \{\Upsilon_j\}\eta_j. \qquad (A18)$$

Thus we have found both the Landau constants and the expansion functions ϕ. In principle this procedure could be carried out to infinity, but in practice a severe truncation would again be applied. With the Landau constants, the ordinary differential equations for the amplitudes and phases can be integrated, and used to construct the velocity field in space and time.